Active and Passive Elec. Comp., 1995, Vol. 18, pp. 23–30
Reprints available directly from the publisher
Photocopying permitted by license only

NANOCRYSTALLINE TiO_2 ELECTRODES EXHIBITING HIGH STORAGE CAPACITY AND STABILITY IN RECHARGEABLE LITHIUM BATTERIES

SUI-YANG HUANG, LADISLAV KAVAN, ANDREAS KAY and MICHAEL GRÄTZEL
Institute of Physical Chemistry, Swiss Federal Institute of Technology, CH-1015, Lausanne, Switzerland

IVAN EXNAR,
Renata SA, CH-4452 Itingen, Switzerland

(Received November 20, 1994; in final form November 30, 1994)

Nanocrystalline TiO_2 films were explored for the first time as electrode material for a rechargeable lithium intercalation cell, i.e., $Li/LiCF_3SO_3 + PC/TiO_2$. Two kinds of nanocrystalline films, TiO_2 F387 (Degussa) and TiO_2 colloid-240, were investigated. These films exhibited excellent performance renderings them a promising choice for secondary battery applications. At a current density of 0.01 mA/cm^2, two voltage plateaus at 1.78 and 1.89 V were observed for TiO_2 F387 films during charge and discharge, respectively. The TiO_2 electrode charge capacity per unit weight rose with decreasing current density. The highest capacity, obtained at a current density of 0.005 mA/cm^2 and a final discharge voltage of 1.4 V, was 265 mAh/g corresponding to a lithium insertion ratio of $x = 0.8$. Nanocrystalline TiO_2 colloid-240 films showed a similar performance. The cycle life of a TiO_2 colloid-240 cell at a high current density was found to be excellent; a capacity loss lower than 14% has been observed over 100 charge/discharge cycles.

1. INTRODUCTION

Over the last 10 years of lithium battery development, much research effort has been focused on $LiMO_2$ (M = Co, Ni, Mn) and TiS_2 lithium insertion compounds.[1–5] These oxides or sulfides are generally employed as positive electrodes in the form of compressed pellets mixed with carbon and a polymeric binder. They consist of particles whose size is in the micron range. The oxide or sulfide crystals contain layers or channels allowing for reversible lithium ion insertion and extraction into and from the host lattice. Apart from the lattice structure, the performance of a lithium battery, i.e., its capacity, cycle life and electric energy storage efficiency, may also depend on the morphology of the host solid, which is related to particle size and surface texture.[6–7] In the present investigation, the suitability of nanocrystalline oxides for use as intercalation electrodes in batteries is explored. These films are distinguished by a very high internal surface area, the roughness factor of a 10-micron-thick layer being of the order of 1000.[8,9] Pores in the nanometer range are present between the oxide

particles. These are interconnected and become filled with electrolyte or a solid hole transmitter. Brief sintering produces efficient contact between the particles. Electronic charges injected in the film from the conducting support are able to percolate rapidly through the entire particle network. Apart from their outstanding performance in dye sensitized photovoltaic cells,[8,9] nanocrystalline films made, for example, of 15 nm sized TiO_2 particles have been shown to intercalate lithium rapidly and reversibly allowing for efficient electrochromic switching of such transparent films.[10]

Titanium dioxide has many advantages compared to the electrode materials mentioned above: (i) its molecular weight is relatively low, hence its theoretical specific charge (336 mAh/g) for $LiTiO_2$ is higher than that of $LiMnO_2$ (285 mAh/g), $LiCoO_2$ (273 mAh/g), $LiNiO_2$ (274 mAh/g) and TiS_2 (239 mAh/g); (ii) it is readily available and cheap; (iii) it is non-toxic and tolerable for the environment. Therefore, TiO_2 is a promising electrode material for the rechargeable lithium battery. In this paper we describe the preparation of TiO_2 nanocrystalline film electrodes and report results obtained from X-ray diffraction, SEM, and electrochemical studies. The effect of current density on the charge storage capacity of such TiO_2 electrodes is analyzed and preliminary results on the cycle life of such rechargeable battery systems are reported.

2. EXPERIMENTAL

2.1. ELECTRODE PREPARATION

Nanocrystalline layers of TiO_2 were prepared from either commercially available TiO_2 powder F 387 (Degussa, Hanau, Germany) or from a colloidal paste (C-240) synthesized in our laboratory.

Titanium dioxide powder F 387 obtained by flame hydrolysis of $TiCl_4$ according to the manufactures specification consists of 90% anatase and 10% rutile. The specific surface area is 82 m^2/g and the main impurity is 0.1% Cl. The powder contains aggregates of primary particles, which have to be dispersed for the preparation of densely packed and well adherent films. This is achieved by grinding with a small amount of water, resulting in high shear forces that disrupt the aggregates. A titanium chelating agent (e.g., acetyl acetone) stabilizes the colloidal particles once they are separated. For the experiments reported here, 0.6 g of F 387 powder were ground in a small porcelain mortar with 0.2 ml water (Millipore purified) and 20 μl acetyl acetone (Merck, p.a.) to yield a highly viscous paste. This was diluted by slow addition of 1.8 ml H_2O under continued griding. Finally, 10 μl Triton X-100 (Fluka, p.a.) was added to improve wetting of the substrate.

The C-240 colloid was synthesized by using a method described elsewhere.[9] The starting material of titanium tetraisopropoxide was slowly hydrolyzed at room temperature and then autoclaved at 240°C at a pressure of 340N/cm^2 for 12 h in a titanium container. To form films, the sol was concentrated by evaporation of water in vacuum at 25°C until a viscous liquid was obtained. Carbowax M-20,000

(40% by weight of TiO_2) was added and the final viscous paste had 20% by weight of TiO_2.

Titanium sheets of 0.5 mm thickness served as conducting substrates for the nanocrystalline layers. They were etched for 30 minutes in boiling HCl (16%, Fluka p.a.), dried, and covered at two parallel edges with Scotch-tape (40 μm thick) in order to provide the desirable thickness of the coating and protect areas for electrical contact. A volume of 5 $\mu l/cm^2$ of the TiO_2 dispersion was applied to one of the free edges and spread over the titanium sheet by a glass rod sliding on the Scotch-tape covered edges. After drying for 10 minutes at room temperature the coatings were sintered in air at 450°C for 10–30 minutes and then dried at 300°C and 10^{-6} torr for 2 hours. The film thickness was between 5 and 10 μm. The sintered and dried layer electrodes were entered directly into a glove box avoiding any air contact. The amount of TiO_2 was determined from the mass difference of the sheet before and after coating.

2.2. ELECTROLYTE SOLUTION

The electrolyte solution was 1 M $LiCF_3SO_3$ dissolved in propylene carbonate (PC). The propylene carbonate (Fluka, 99%) was purified by fractional distillation under vacuum and dried over a 4 Å molecular sieve. $LiCF_3SO_3$ (Fluka) was dried at 150°C and 10^{-6} torr during 72 hours. The water content in the prepared electrolyte solution was below 20 ppm, as determined by Karl-Fischer titration.

2.3. CHARACTERIZATION

The starting powder and films were characterized by X-ray diffraction (XRD). XRD data was obtained by using an X-ray diffractometer Siemens DS500 with Cu$K\alpha$ radiation.

The morphology of the samples was analyzed by Scanning Electron Microscopy (SEM) using a Hitachi S-900 instrument.

2.4. ELECTROCHEMICAL TESTING

Electrochemical experiments employed a conventional three-electrode cell interfaced to a computer-aided potentiostatic/galvanostatic set-up (PAR EG & G model 273 A). A one-compartment (diaphragmless) cell was used with the electrolyte solution volume about 15 ml. The reference and auxiliary electrodes were prepared from pure lithium (Aldrich). All experiments were performed in an argon-filled glove box (JACOMEX BS531) whose atmosphere contained less than 5 ppm H_2O and 6 ppm O_2.

3. RESULTS AND DISCUSSION

Fig. 1 shows the XRD patterns of the TiO_2-F387 film as well as of its starting powder, and the nanocrystalline TiO_2 film produced from the C-240 colloid. The diffraction patterns can be attributed to the presence of anatase and rutile phases. In the case of TiO_2-F 387, the ratio of diffractional intensity indicates a 9:1

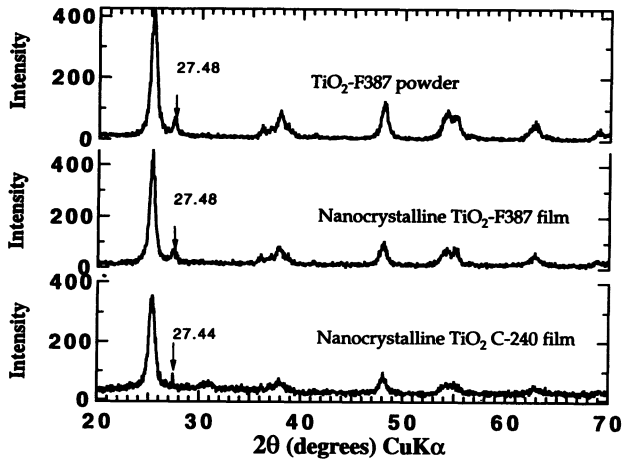

FIGURE 1 XDR diagrams of the TiO_2-F387 (Degussa) powder, F387 (Degussa) and colloidal TiO2 C-240 films. The arrows indicate the intense rutile lattice diffraction with 2θ values.

proportion of anatase to rutile. There is no obvious change of the XRD spectra between powder and sintered layers. The film of TiO_2-colloid presents practically pure anatase phase.

The primary particle size can be estimated by using the Scherrer equation:

$$D = 0.9\lambda/\beta_{1/2} \cos\theta$$

where λ is the X-ray wavelength, $\beta_{1/2}$ the corrected width of the main diffraction peak at half height and θ the diffraction angle. The D values found for the F387 powder, the F387 film, and the C-240 film are 12 nm, 13 nm and 10 nm, respectively, indicating that the sintering has practically no influence on the particle size.

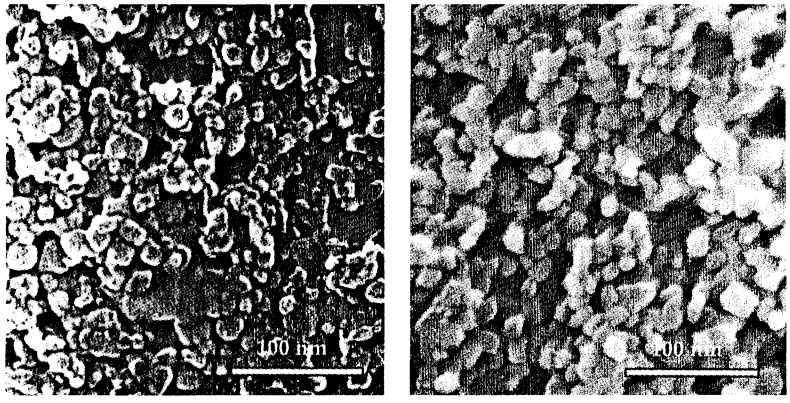

FIGURE 2 Top view SEM micrographs of the TiO_2-F387 (a) and TiO_2-C-240 films (b).

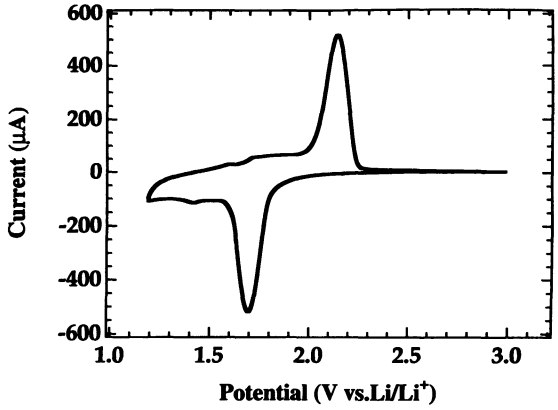

FIGURE 3 Cyclic voltammogram obtained with a nanocrystalline F-387 (Degussa) film electrode in 1 M $LiCF_3SO_3$-propylene carbonate electrolyte. Electrode area 0.95 cm^2, mass of TiO_2 1.803 mg, scan rate 0.1 mV/s.

Typical SEM micrographs of the TiO_2-F387 and C240-films are shown in Fig. 2. The electrodes are highly textures with open pores and channels. The particle size is about 10–15 nm, in accord with the XRD results.

Fig. 3 shows a cyclic voltammogram obtained with the TiO_2-F387 film electrode in the presence of 1 M $LiCF_3SO_3$ electrolyte. The pronounced cathodic and anodic peaks are due to lithium insertion and release respectively. The total cell reaction on discharge and charge is given by the equation:

$$TiO_2 + xLi^+ + xe^- \underset{\text{charge}}{\overset{\text{discharge}}{\rightleftharpoons}} Li_xTiO_2.$$

The voltammetric charge determined by integration of the voltammetric peaks equals 152.05 mAh/g and 197.65 mAh/g for the anodic and cathodic process, respectively. The corresponding stoichiometric coefficients are $x = 0.45$ and $x = 0.59$ for lithium release and insertion, respectively. The anodic charge is likely to present more reliable measure for the Li insertion stoichiometry, since cathodic breakdown of the electrolyte solution might obscure the true insertion currents at potentials below 1.5 V. Voltammograms obtained with the C-240 colloidal film exhibit very similar features to Fig. 3.

Fig. 4 presents galvanostatic discharge/charge curves measured over three cycles for the $Li/LiCF_3SO_3 + PC/TiO_2$-F387 cell. Experiments were carried out at a current density of 0.01 mA/cm^2. The freshly assembled device has an open-circuit potential of about 3 V. For the first cycle, the final discharge potential was 1.5 V while for the other two cycles, it was selected to be 1.4 V. Voltages smaller than 1.4 V were avoided to prevent cathodic decomposition of the electrolyte. During the discharging and charging process, pronounced voltage plateaus occur at 1.78 and 1.89 V, respectively, their difference presenting the overvoltage loss. From the ratio of the discharge and charge capacity one derives a reversibility of 97% for the cut-off voltage 1.5 V and 91–93% for the cut-off voltage 1.4 V. This charge unbalance is apparently caused by the cathodic decom-

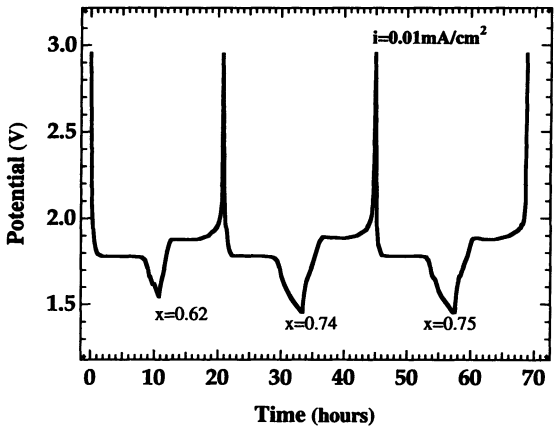

FIGURE 4 Amperostatic discharge/charge curves obtained with a nanocrystalline $Li/LiCF_3SO_3$, PC/Li_xTiO_2-F387 film cell, current density was 0.01 mA/cm^2.

position of PC and trace water at low cathodic potentials. However, these results render this type of device attractive for high energy charge and storage secondary battery applications.

Fig. 5 illustrates galvanostatic cycling of the same cell at different current densities. As expected, the overvoltage losses increase with current density, although the effect is small within the range investigated.

The variation of the charge storage capacity of the nanocrystalline TiO_2 electrodes with current density is shown in Fig. 6 for final discharge potentials of 1.4 and 1.5 V. The charge storage capacity increases with decreasing current density. The highest charge storage capacity was obtained by using a current density of 5 $\mu A/cm^2$ where $C = 265$ mAh/g corresponding to a Li insertion ratio of

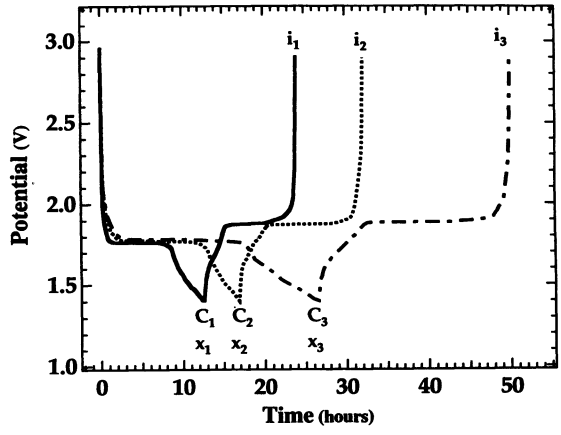

FIGURE 5 Amperostatic discharge/charge curves obtained with nanocrystalline $Li/LiCF_3SO_3$, PC/Li_xTiO_2-F387 ($m = 0.5$ mg) film cells using different current density: $i_1 = 0.01$ mA/cm^2($C_1 =$ 248 mAh/g, $x_1 = 0.74$); $i_2 = 0.0075$ mA/cm^2 ($C_2 = 251$ mAh/g, $x_2 = 0.76$); $i_3 = 0.005$ mA/cm^2 ($C_3 = 265$ mAh/g, $x_3 = 0.80$).

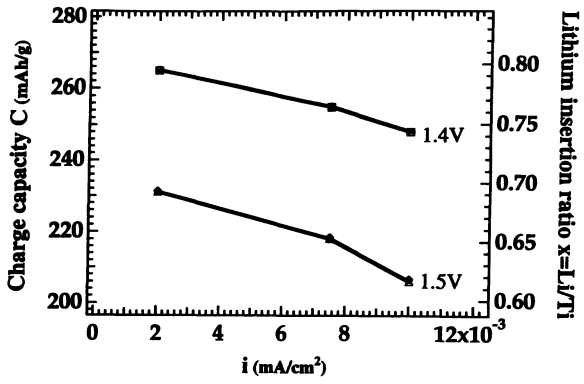

FIGURE 6 Effect of current density on the charge storage capacity of nanocrystalline $Li/LiCF_3SO_3 + PC/Li_xTiO_2$-F387 film cells, derived from the discharge process. The indicated values are the final discharge voltage.

$x = 0.8$. The theoretical limit for $x = 1$ is 336 mAh/g. Based upon the weight of the active electrode material and the discharge potential 1.78 V, the cell delivered a specific energy density of 472 Wh/kg (theoretical one is 598 Wh/kg).

Finally, the cycling performance of a $Li/LiCF_3SO_3 + PC/TiO_2$-C-240 film cell is shown in Fig. 7. The cell was discharged and charged between 1.5 and 3.0 V at a relatively high current density of 0.2 mA/cm^2 in order to make the cyclelife test in a reasonable time. The cell delivered an initial charge capacity of 108.8 mAh/g, corresponding to $x = 0.3$, the cell capacity loss being less than 14% for over 100 cycles. A visual inspection of the used electrodes showed mechanical cracks in the film. We suspect that the capacity loss may be due to the loss of interparticle electrical contacts. The electrolyte decomposition, mentioned above, is presummably less significant since the test was performed with an excess of the electrolyte solution.

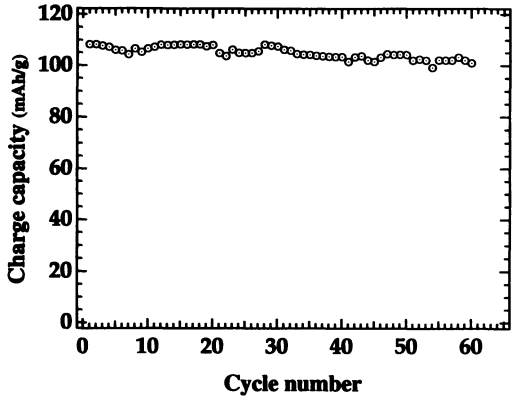

FIGURE 7 Charge storage capacity of a $Li/LiCF_3SO_3$,PC/TiO_2C-240 cell under continuous cycling at the relatively high current density of 0.2 mA/cm^2. The film mass was 1.47 mg.

4. CONCLUSIONS

The present study establishes the promising performance of nanocrystalline transition metal oxides in lithium intercalation batteries. The specific porous morphology of such films offers the advantage of providing a very large internal surface area facilitating lithium exchange between the solid and electrolyte phase. This allows insertion and release of the Li ions to occur rapidly and reversibly. These characteristics paired with stable performance under repeated cycling render nanocrystalline oxides particularly attractive for secondary battery applications.

ACKNOWLEDGMENTS

The authors wish to thank Dr. Pedro Moeckli (Laboratoire de céramiques, DMX, Swiss Federal Institute of Technology) for his contribution to the X-ray analysis of the samples and Dr. V. Shklover (Institute of Crystallography and Petrography, ETH Zürich) for SEM observations. This work is sponsored by CERS (Commission pour l'encouragement de la recherche scientifique, Berne, Switzerland). Their financial support is gratefully acknowledged. Useful discussions with Dr. J. P. Randin (ASULAB SA) are greatly appreciated.

REFERENCES

1. K. Mizushima, P.C. Jones, P.J.Wiseman and J. B. Goodenough, Solid State Ionics, 3–4, 171, (1981).
2. C. Delmas, J. Braconnier, A. Maazaz and P. Hagenmuller, Rev. Chem. Miner., 19, 343 (1982).
3. J. Molenda, Solid State Ionics, 21, 263 (1986).
4. E.J. Plichta and W.K. Behl, J. Electrochem. Soc., 140, 46 (1993).
5. F. Croce, S. Passerini and B. Scrosati, J. Electrochem. Soc., 141, 1405 (1994).
6. S.D. Han, N. Treuil, G. Campet, J. Portier, C. Delmas, J.C. Lassègues and A. Pierre, Active and Passive Electron. Compon. (in press).
7. S.D. Han, Ph.D. thesis of the University of Bordeaux (1994).
8. B. O'Regan, J. Moser, M. Anderson and M. Grätzel, J. Phys. Chem., 94, 8720 (1990).
9. B. O'Regan and M. Grätzel, Nature, 353,24,737 (1991).
10. A. Hagfeldt, N. Vlachopoulos and M. Grätzel, J. Electrochem. Soc., 141, 7, L82 (1994).